



available at [www.sciencedirect.com](http://www.sciencedirect.com)



journal homepage: [www.elsevier.com/locate/jhydrol](http://www.elsevier.com/locate/jhydrol)



# Estimated changes in flood quantiles of the river Meuse from resampling of regional climate model output

Robert Leander <sup>a,\*</sup>, T. Adri Buishand <sup>a</sup>, Bart J.J.M. van den Hurk <sup>a</sup>,  
Marcel J.M. de Wit <sup>b</sup>

<sup>a</sup> Royal Netherlands Meteorological Institute (KNMI), P.O. Box 201, 3730 AE De Bilt, The Netherlands

<sup>b</sup> The Dutch Directorate for Public Works and Water Management, P.O. Box 17, 8200 AA Lelystad, The Netherlands

Received 2 February 2007; received in revised form 10 December 2007; accepted 18 December 2007

## KEYWORDS

Meuse basin;  
Regional climate  
models;  
Nearest-neighbour  
resampling;  
Hydrological modelling;  
Extreme values;  
Climatic change

**Summary** Precipitation and temperature data from three regional climate model (RCM) experiments were used to assess the effect of climatic change on the flood quantiles of the French–Belgian river Meuse. In two of these experiments the RCM was driven by the global atmospheric model HadAM3H of the Hadley Centre (HC), and in the other experiment the RCM was driven by the global coupled atmosphere–ocean model ECHAM4/OPYC3 of the Max-Planck Institute for Meteorology (MPI). RCM simulations for the control climate (1961–1990) and the SRES-scenario A2 (2071–2100) were available. The HBV rain-fall–runoff model was used to simulate river discharges. Long synthetic sequences of precipitation and temperature were resampled from the RCM output using a nearest-neighbour technique to obtain the flood quantiles for long return periods. The maxima of 10-day precipitation and discharge for the winter half-year (flooding season) were analysed. It was found that the changes in the extreme quantiles of 10-day precipitation and discharge were highly sensitive to the driving GCM. In the runs driven by HC, there was little change in the most extreme quantiles, whereas the MPI-driven run projected a remarkable increase. It is shown that this difference between the HC- and MPI-driven runs is strongly related to the change in the coefficient of variation of the 10-day precipitation amounts, which decreases in the former and hardly changes in the latter. The relevance of bias correction of RCM output with regard to the estimated changes of flood quantiles is demonstrated.

© 2008 Elsevier B.V. All rights reserved.

\* Corresponding author. Tel.: +31 302206429; fax: +31 302210407.  
E-mail address: [leander@knmi.nl](mailto:leander@knmi.nl) (R. Leander).

## Introduction

From the perspective of policy making the interest in the impacts of local climatic change on river flows is increasing. It is generally believed that climate change will lead to increased flooding in many areas (Kay et al., 2006). For the Netherlands potential changes in the statistics of extreme flows are highly relevant, since the major part of the country is situated in the delta of the rivers Rhine and Meuse.

Most of the research on the impact of climate change on river discharges in the Netherlands relates to the river Rhine. To assess the impact of climate change on the monthly mean and peak discharges of the river Rhine, Kwadijk and Rotmans (1995) applied gridded patterns of changes in temperature and precipitation, obtained from seven equilibrium experiments with general circulation models (GCMs), to the observed monthly precipitation and temperature and used the perturbed data to drive a distributed hydrological model (RHINEFLOW) for the river basin. The same approach was followed in a study coordinated by the International Commission for the Hydrology of the Rhine Basin (CHR) using the output from one transient and two equilibrium GCM experiments (Grabs, 1997; Middelkoop et al., 2001). As in Kwadijk and Rotmans (1995), the effect of climate change was calculated by applying the changes found in the GCM experiments to the baseline climate and RHINEFLOW was used at a monthly resolution for the rainfall–runoff modelling of the Rhine basin. The assessment of the changes in river discharges was limited to the mean annual cycle at different gauging stations. In a later study (Middelkoop, 2000) the RHINEFLOW model was operated at a temporal resolution of 10 days, using data from the UKHI GCM of the Hadley Centre of the UK Met Office. Shabalova et al. (2003) were the first to use data from a regional climate model (RCM) to assess the impact of climate change on the discharges of the river Rhine in the Netherlands. They used HadRM2 of the Hadley Centre nested within the global coupled climate model HadCM2. The changes in 10-day precipitation and temperature were applied to the observed baseline series. Using RHINEFLOW, it was found that the changes in extreme 10-day flows were very sensitive to the type of transformation (linear or nonlinear) applied to the precipitation amounts. This sensitivity was also observed in a study of Prudhomme et al. (2002) for the Severn catchment (UK). Lenderink et al. (2007) investigated the direct use of bias-corrected 10-day HadRM3H regional climate model data (also from the Hadley Centre) as input to RHINEFLOW. They compared the changes in discharge with those obtained by perturbing the RCM control run. One of their findings was that direct use of RCM data should be preferred if other discharge characteristics than the mean (such as extremes) are of interest.

Several other studies have been performed for individual subbasins of the river Rhine upstream of the Netherlands. A number of relatively small subbasins were considered in the CHR study described by Grabs (1997) and Middelkoop (2000). Detailed hydrological models were used to estimate climate change impacts. As in the RHINEFLOW application to the entire river basin, scenarios for future climate were obtained by perturbing the baseline climate with the changes from three GCM experiments. Bárdossy and Zehe (2002) studied

the impact of climate change on floods and the runoff regime of the major German subbasins of the river Rhine, using a stochastic downscaling technique for generating daily precipitation and temperature, conditional on the circulation patterns of a control and a scenario run of the ECHAM4 GCM, and the semi-distributed HBV model (Lindström et al., 1997) for hydrological simulations. Kleinn et al. (2005) nested the distributed hydrological model WaSiM-ETH for the Rhine upstream of Cologne into a cascade of two versions of the Swiss/German regional climate model CHRM (with respective spatial resolutions of 14 km and 56 km). The 56-km model was driven by observed lateral boundary conditions from a 5-year ECMWF reanalysis. Future climate conditions were not considered in that study.

For the Meuse basin an extensive study has been carried out by Booij (2002, 2005). He used a first order Markov chain to generate a time series of daily basin-average precipitation and developed a discrete random cascade model for spatial disaggregation of precipitation. The parameters of the Markov chain for the current and the future climate were obtained from transient runs of three GCMs (CGCM1, HadCM3 and CSIRO9) and two RCMs (HadRM2 and HIRHAM4). The parameters for the cascade model were estimated from the two RCMs. HBV was used for the hydrological simulations. A subdivision of the Meuse basin into 15 subbasins was compared with a subdivision into 118 subbasins and no subdivision. de Wit et al. (2007) analysed the impact of climate change on the occurrence of low flows in the river Meuse, using RCM simulations from the EU-funded PRUDENCE (Prediction of Regional scenarios and Uncertainties for Defining European Climate change risks and Effects) project, see e.g. Christensen and Christensen (2007). Their study indicates that climate change will lead to a decrease in the average discharge of the Meuse during the low flow season. Considerable problems were, however, encountered with the simulation of critical low flow conditions of the Meuse. Bultot et al. (1988) and Gellens and Roulin (1998) investigated the impact of climate change for some Belgian subbasins of the river Meuse by perturbing the baseline climate.

Leander and Buishand (2007), from here LB07, presented a detailed study of bias correction of RCM output for the Meuse basin. They also applied nearest-neighbour resampling to obtain long sequences of daily precipitation and temperature required to simulate long-duration series of river flows. The study was restricted to two experiments with the KNMI regional climate model RACMO under current climate conditions. The simulated series were successfully used to estimate flood quantiles for return periods far beyond the extent of the original RCM runs. Therefore, this approach offers a possibility to estimate extreme flood quantiles for a future climate using data from scenario runs.

In this study the methodology presented and tested in LB07 is employed to assess the effects of RCM climate change projections on rare flood quantiles. In that sense, it is a continuation of the work presented in LB07. It could also be regarded as an extension of the work done by Lenderink et al. (2007), because it demonstrates a new way to take advantage of RCM output for the investigation of rare flood quantiles, by using a resampling method and a more sophisticated bias correction. Furthermore, the hydrological model is operated at a

daily, rather than a 10-day timestep. Three RCM–GCM configurations are considered. Since for rivers like the Meuse the occurrence of extreme flows depends strongly on the variability and the extremes of multi-day precipitation amounts (Tu (2006) mentions durations between 7 and 10 days), the statistics of 10-day precipitation amounts receive much attention.

First, a description of the study area is given and the RCM–GCM configurations, the nearest-neighbour resampling scheme and the rainfall–runoff model are discussed. This is followed by an explanation of the bias correction of RCM output and its implications for the three RCM–GCM configurations. Then the changes in precipitation and temperature characteristics, found by comparing the control and scenario runs, are discussed with particular attention to the quantiles of extreme 10-day precipitation amounts. Subsequently, the simulated changes of flood quantiles resulting from the hydrological simulations are presented. Finally, the results are summarized and some concluding remarks are made.

## Study area, models and methods used

The river Meuse is the second largest river in the Netherlands. It originates in the north-east of France and traverses the Belgian Ardennes, which is the source of a major portion of its discharge. The gauging station Borgharen, considered in this study, is located near the Belgian–Netherlands border (drainage area  $\approx 21,000 \text{ km}^2$ ). The mean discharge at this gauging station ranges from  $100 \text{ m}^3 \text{ s}^{-1}$  in September to about  $500 \text{ m}^3 \text{ s}^{-1}$  in January. This strong seasonal cycle can mainly be ascribed to that of the evapotranspiration (de Wit et al., 2007).

For 15 subbasins the daily area-average precipitation was available for the historical period 1961–1998. These data were obtained from the Royal Meteorological Institute of Belgium for the Belgian subbasins and calculated from station data (63 stations) for the French subbasins. Daily potential evapotranspiration (PET) data were available for the Belgian subbasins for the period 1967–1998. The PET values for the French subbasins were set equal to the area-weighted average of the Belgian subbasins. This is justified by the fact that in the flood situations of interest PET only plays a minor role. Daily temperature was available for 11 stations in and around the Meuse basin. Three RCM–GCM configurations are considered in this study. One consists of the regional climate model RACMO of KNMI (Lenderink et al., 2003), driven by the high-resolution global atmospheric model HadAM3H (Jones et al., 2001) of the Hadley Centre. In the other two configurations the regional climate model RCAO (Räisänen et al., 2004) of the Swedish Meteorological and Hydrological Institute (SMHI) was used, either coupled to HadAM3H or the global atmosphere–ocean model ECHAM4/OPYC3 of the Max-Planck-Institute of Meteorology (MPI) in Hamburg, Germany (Roeckner et al., 1999), also used by Bárdossy and Zehe (2002). These model configurations are from here denoted as RACMO-HC, RCAO-HC and RCAO-MPI, respectively.

The specific choice of RCM runs and driving GCMs allows for a distinction between effects related to the driving GCM and those produced by the RCM itself. For each configura-

tion two runs were considered, one for the control period 1961–1990 and one for the period 2071–2100, based on the SRES-scenario A2. These RCM runs were performed in the framework of the PRUDENCE project (Jacob et al., 2007). RCAO and RACMO have a resolution of  $\approx 50 \text{ km}$  over the Meuse basin, which is located near the centre of their domains. From both models 15 grid boxes were selected which almost entirely cover the basin (Fig. 1).

The main goal of the current study is to investigate events with return periods in the order of 1000 years, relevant to the design water levels of the embanked part of the river Meuse in the Netherlands. Since the model runs all have a length of only 30 years, this requires strong extrapolation, introducing large uncertainties in precipitation and flood quantiles to be estimated. Therefore, a data-driven weather generator was used in this study to generate long-duration time series of precipitation and temperature. This weather generator is based on nearest-neighbour resampling and uses precipitation and temperature data from the RCM integrations. The algorithm implemented for this study essentially samples days from the model runs with replacement. The selection of a day being added to the synthetic sequences is conditioned on the spatially averaged standardized precipitation and temperature of the last

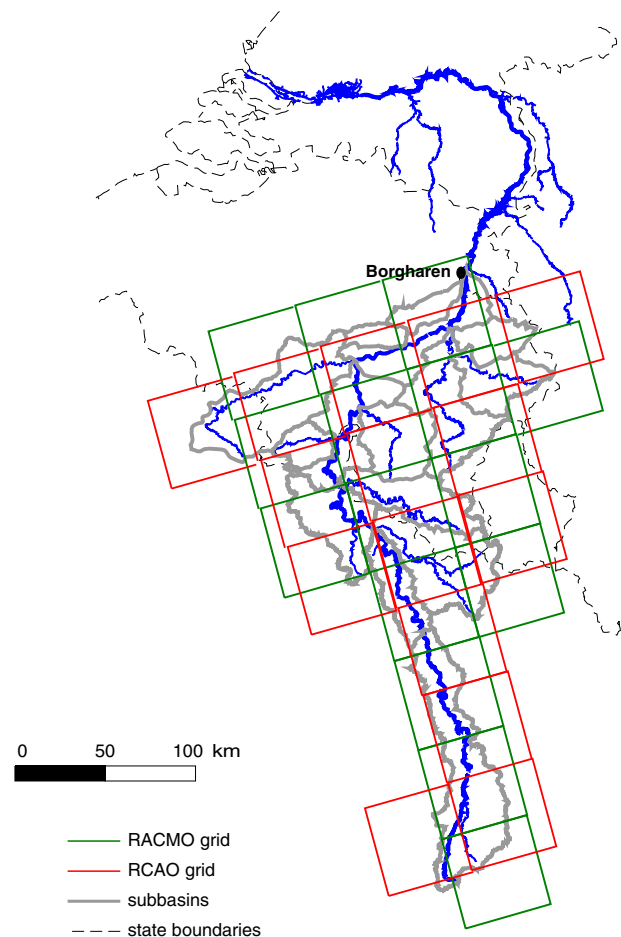


**Figure 1** Locations of the 15 used grid boxes of RACMO (green) and those of RCAO (red), relative to the Meuse subbasins (grey).

added day and the precipitation total of its five predecessors. The general principles of nearest-neighbour resampling and the application to daily precipitation and temperature are described in Rajagopalan and Lall (1999). One of the features of the algorithm is that it is capable of reproducing the daily variability and persistence in the underlying data, and hence the variability of multi-day aggregates (Leander et al., 2005). Besides, the spatial correlation of precipitation and temperature and the correlation between those two variables on a daily resolution are preserved by definition. Therefore, it is a particularly suitable tool in the study of extreme discharges. More on the specific implementation of the algorithm used in this study can be found in Leander et al. (2005) and LB07.

For rainfall–runoff modelling the semi-distributed HBV model, developed at SMHI, was used (Lindström et al., 1997). The Meuse basin upstream of Borgharen was divided into 15 subbasins, depicted in Fig. 1. Beside daily precipitation and temperature, the HBV model also requires daily PET for each subbasin. In the simulations with observed meteorological data the available observed PET values were used. For the simulations with RCM data, daily PET was derived from the (bias-corrected) daily temperature  $T$  using the relation:

$$\text{PET} = [1 + \alpha_m(T - \bar{T}_m)] \overline{\text{PET}}_m, \quad (1)$$

with  $\bar{T}_m$  the mean observed temperature (°C) and  $\overline{\text{PET}}_m$  the mean observed PET (mm/day) for calendar month  $m$  in the period 1967–1998. As in LB07, the proportionality constant  $\alpha_m$  was determined for each calendar month by means of a regression of the observed PET value for the Belgian part of the basin on the observed daily temperature. An elaborate description of the HBV model and its application to the Meuse basin can be found in Booij (2005).

## Bias correction of RCM data

In LB07 the precipitation bias in the control simulation of RACMO-HC for the study area was discussed. Table 1 summarizes the performance of the used model configurations for the Meuse basin for the winter as well as the summer half-year. The observations for the 30-year period 1969–1998 were used as a reference. This period was also considered in LB07. All three model runs show a positive bias in the mean precipitation, in particular RCAO-MPI. This bias is mainly related to that of the fraction  $f_{\text{wet}}$  of wet days ( $\geq 0.3$  mm), because the mean wet-day amount  $m_{\text{wet}}$  is fairly well reproduced. The left panel of Fig. 2 shows the basin-average relative precipitation bias for each calendar month. RACMO-HC and RCAO-HC have similar biases, whereas RCAO-MPI has a much larger bias in the months July–October. The large positive bias in this part of the year is characteristic for control simulations driven by MPI for western Europe and is possibly related to a positive bias in the westerlies (van Ulden et al., 2007). Furthermore, the coefficient of variation (CV) of daily precipitation ( $\text{CV}_1$ ) is too low in all RCM runs. This is also the case for the CV of the 10-day precipitation amounts (not shown).

The lag 1 autocorrelation coefficient  $r_1$  in winter is overestimated by RCAO-HC and slightly underestimated in the

**Table 1** Performance of the three model configurations for precipitation during the winter half-year (October–March) and the summer half-year (April–September)

	Obs.	RACMO-HC	RCAO-HC	RCAO-MPI
<i>Winter</i>				
Mean (mm/day)	2.77	3.49	3.25	3.58
$\text{CV}_1$	1.73	1.48	1.36	1.26
$r_1$	0.37	0.35	0.40	0.35
$f_{\text{wet}}$ (%)	56	68	70	76
$m_{\text{wet}}$ (mm/day)	4.94	5.10	4.60	4.72
<i>Summer</i>				
Mean (mm/day)	2.40	2.64	2.58	2.97
$\text{CV}_1$	1.81	1.69	1.69	1.54
$r_1$	0.27	0.25	0.31	0.22
$f_{\text{wet}}$ (%)	50	57	56	63
$m_{\text{wet}}$ (mm/day)	4.75	4.58	4.52	4.69

The mean daily amount, the coefficient of variation  $\text{CV}_1$ , the lag 1 autocorrelation coefficient  $r_1$ , the fraction  $f_{\text{wet}}$  of wet days and the mean wet-day amount  $m_{\text{wet}}$  are area-weighted averages over all subbasins.

other two model configurations. In summer the same is found, though the differences between the models and the observations are somewhat larger.

A linear scaling of precipitation does not correct the underestimation of  $\text{CV}_1$  or that of the multi-day CVs. It was shown by LB07 that this can have undesirable effects on large quantiles of multi-day precipitation. Hence, such a correction is unsuited for any study of extreme precipitation and simulated discharge. A slightly more advanced non-linear correction in the form:

$$P^* = aP^b \quad (2)$$

was introduced in LB07 to correct the variability as well as the mean precipitation. The seasonally and spatially varying (i.e. among subbasins) parameters  $a$  and  $b$  were determined for each interval of five calendar days in the year by considering days within a moving window of 65 days centred on the 5-day period of interest. For each window the values of  $a$  and  $b$  were chosen such that the mean precipitation and the CV of 10-day precipitation amounts ( $\text{CV}_{10}$ ) matched those of the corresponding days from the observed precipitation. Fig. 3 shows how the basin-average exponent  $b$  varies throughout the year for all three control simulations. As observed for the biases in the mean precipitation, there is a strong resemblance between the values of  $b$  for the two HC-driven simulations. For the RCAO-MPI simulation the values of  $b$  are considerably higher. In particular in the months September–November (roughly between day 240 and day 330) the values of the exponent are rather large. It was suspected that these large values were related to the positive bias in  $f_{\text{wet}}$ . To investigate this, the bias in  $f_{\text{wet}}$  was removed prior to the nonlinear correction. A small, seasonally varying reduction was applied to the wet-day precipitation amounts, such that the fraction of days with precipitation amounts above the wet-day threshold (of 0.3 mm) matched the observed  $f_{\text{wet}}$ . Negative precipitation amounts were set to zero. Though this adjustment resulted in smaller values of the exponent  $b$ , the reduction was only marginal.

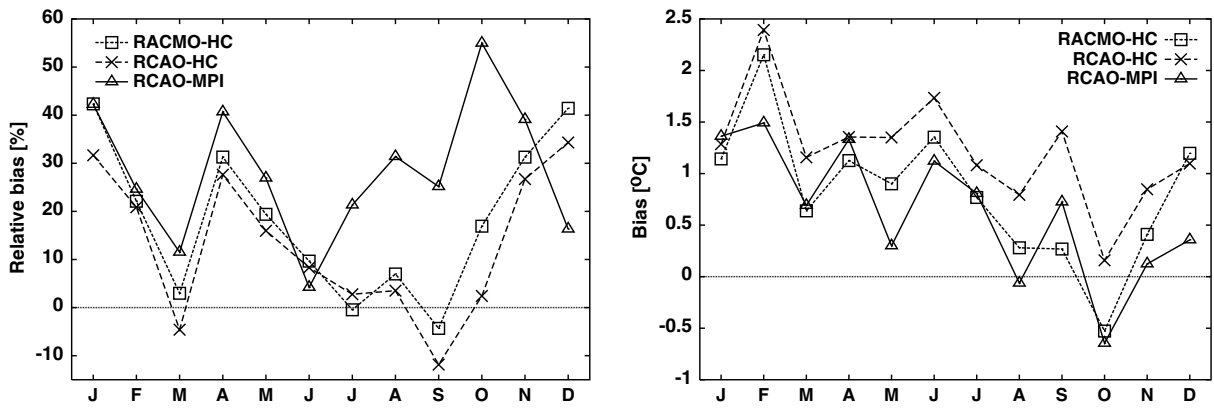


**Figure 2** Basin-average relative bias in the monthly precipitation (left) and the absolute bias in the mean monthly temperature (right) for the control simulations of RACMO-HC (squares), RCAO-HC (crosses) and RCAO-MPI (triangles) for the period 1961–1990. Biases are calculated with respect to the observed means for the period 1969–1998.

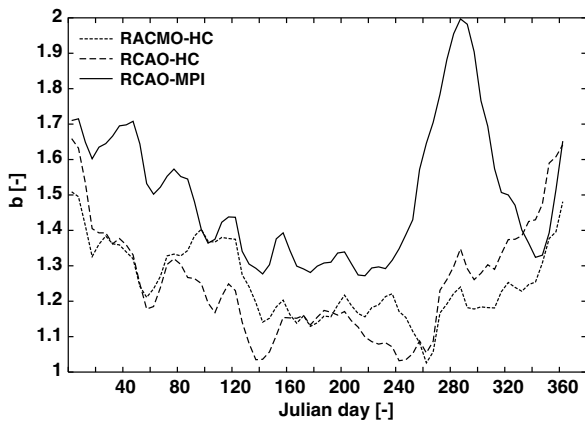


**Figure 3** Annual cycle of the area-averaged correction parameter *b* for RACMO-HC, RCAO-HC and RCAO-MPI.

The right panel of Fig. 2 shows the absolute monthly temperature biases. These were obtained by comparing the basin-average temperature calculated from the grid boxes with the reference temperature for the basin, obtained from data of 11 stations using Thiessen interpolation. For

the three configurations the temperature biases are roughly of the same order, though the bias of RCAO-HC is on average larger than that of the other two model configurations. The daily temperatures of the subbasins were corrected in the same way as in LB07, involving a translation and a scaling, which respectively adjust the mean and the variability. The same translation and scale factor were used for all subbasins, but these parameters were determined separately for each 5-day interval in the year, again using a moving window of 65 calendar days.

### Changes of temperature and precipitation in the RCM runs

For each model configuration precipitation and temperature for the Meuse basin in the A2-scenario run were compared with those in the control run. The left panel of Fig. 4 displays the relative change of the mean precipitation. All model configurations show an increase in winter and a decrease in summer. The changes in RCAO-MPI are the largest in magnitude, ranging from a decrease of about 70% in August to an increase of 60% in December. The decrease in summer precipitation is accompanied by a strong decrease in the

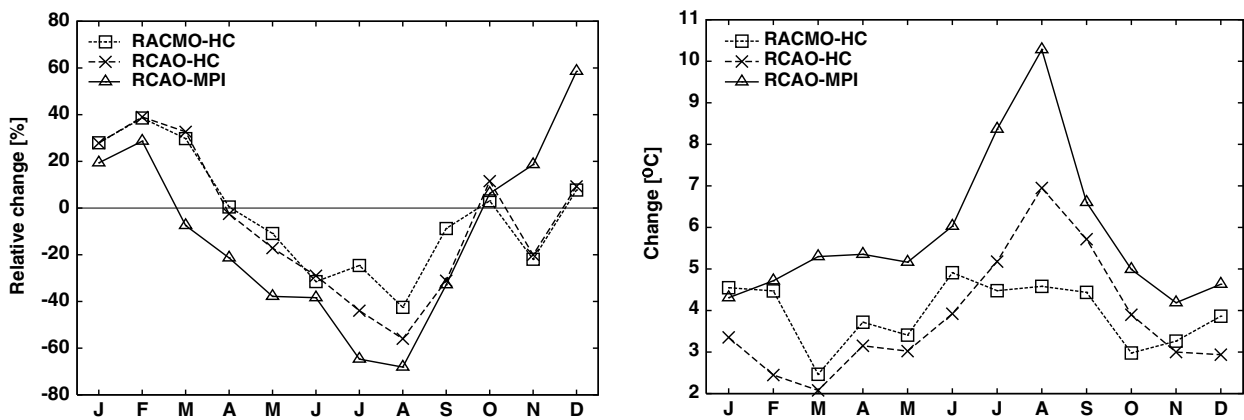


**Figure 4** Relative change in the monthly precipitation (left) and the absolute change in the monthly mean temperature (right), resulting from the A2 scenario, as projected by RACMO-HC, RCAO-HC and RCAO-MPI.

number of wet days (30–50% in the summer months June–August). In winter the change in precipitation frequency is small, but there is a clear increase in the mean wet-day amounts. For December–February, this increase ranges from 16% for the HC-driven runs up to 32% for RCAO-MPI.

The right panel of Fig. 4 displays the change of the mean monthly temperature. Throughout the entire year an increase is found in all model configurations. The changes in both HC-driven runs do not differ much, except for August and September, where RCAO-HC shows a considerably larger increase. This is probably related to the drying-out of the soil, the effects of which can also be seen in the precipitation in the summer months. In the RACMO model several modifications of the soil scheme were made to reduce the positive feedback between soil moisture and temperature. The soil depth was increased, the response of the evapotranspiration to the available soil moisture was modified and the percolation of soil water to deeper layers was reduced. Furthermore, the cloud scheme was altered to increase the cloud cover in summer (Lenderink et al., 2003). In RCAO-MPI the change of the temperature in the summer months is even larger than in RCAO-HC, especially in August, which shows an increase of more than 10 °C.

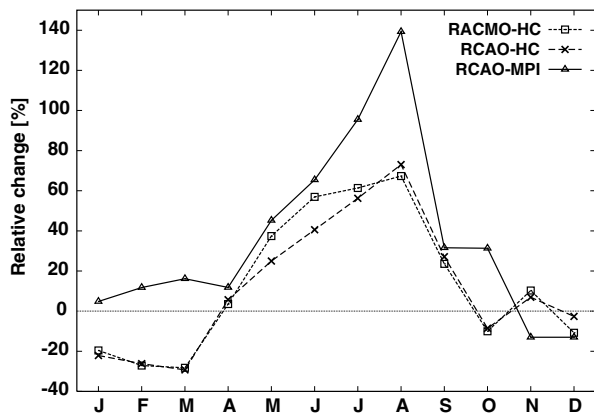
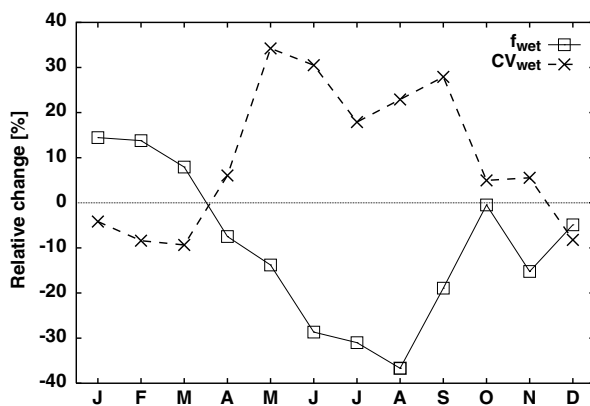


Figure 5 Relative change of  $CV_{10}$  for each calendar month.



In Fig. 5 the relative change of  $CV_{10}$  is shown for all model configurations. The close correspondence between both HC-driven runs (except for May and June) suggests a strong influence of the driving GCM. For RACMO-HC and RCAO-HC the change in winter is comparable to that found by Buishand and Lenderink (2004) for the Rhine basin, using an RCM from the Hadley Centre also driven by HadAM3H boundaries. They observed a decrease of 16% for the months December–February. In summer the relative change shown in Fig. 5 is larger than the relative change found by Buishand and Lenderink (2004).

The change in  $CV_{10}$  can be understood from the changes in certain basic statistical properties of the daily precipitation amounts. For a stationary daily sequence the variance of 10-day totals,  $V_{10}$ , and the variance of daily amounts,  $V_1$ , are related through (Cox and Lewis, 1966, p. 72):

$$V_{10} = 10V_1 \left( 1 + 2 \sum_{i=1}^9 r_i \frac{10-i}{10} \right), \quad (3)$$

where  $r_i$  denotes the lag  $i$  autocorrelation coefficient. Dividing both sides by the squared mean 10-day amount leads to the following expression for  $CV_{10}$ :

$$CV_{10}^2 = \frac{CV_1^2}{10} \left( 1 + 2 \sum_{i=1}^9 r_i \frac{10-i}{10} \right) \quad (4)$$

For  $CV_1$  Räisänen (2002) derived

$$CV_1^2 = \frac{CV_{\text{wet}}^2 + 1}{f_{\text{wet}}} - 1 \quad (5)$$

where  $CV_{\text{wet}}$  is the CV of the wet-day precipitation amounts. From the last two equations it can be seen that  $CV_{10}$  decreases with the number of wet days and increases with  $CV_{\text{wet}}$  and the autocorrelation coefficients. Fig. 6 shows the relative change of  $f_{\text{wet}}$  and  $CV_{\text{wet}}$  (left panel) and the relative change of  $CV_1$ ,  $CV_{10}$  and  $r_{123} = r_1 + r_2 + r_3$  (right panel) for the RACMO-HC run. From the latter it is seen that the direction of change of the autocorrelation coefficients determines whether or not the change of  $CV_{10}$  exceeds that of  $CV_1$  (in accordance with Eq. (4)). In January–March  $f_{\text{wet}}$  increases and  $CV_{\text{wet}}$  decreases, resulting in a decrease of  $CV_1$ . This effect is accompanied by a decrease of the auto-

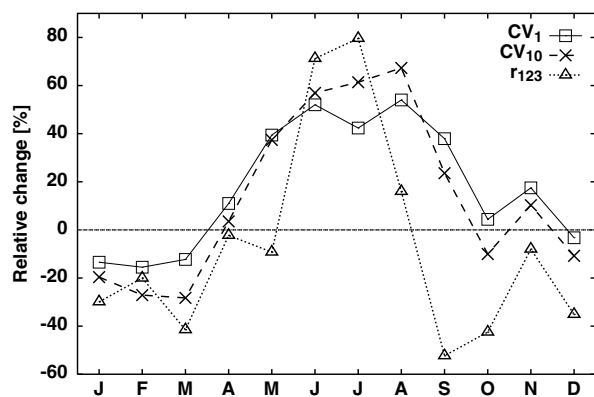


Figure 6 Relative change of  $f_{\text{wet}}$  and  $CV_{\text{wet}}$  for RACMO-HC (left panel) and the corresponding relative change of  $CV_1$ ,  $CV_{10}$  and the sum of the first three autocorrelation coefficients  $r_{123}$  (right panel).

correlation, leading to a larger decrease for  $CV_{10}$  than for  $CV_1$ . The rather large increase of  $CV_{10}$  for the months June–August ( $\approx 60\%$ ) can be attributed to an increase of  $CV_{\text{wet}}$  and the strength of the autocorrelation in combination with a decrease of  $f_{\text{wet}}$ .

The seasonal changes of  $f_{\text{wet}}$ ,  $CV_{\text{wet}}$  and the autocorrelation in RCAO-HC are similar to those in RACMO-HC. The results for RCAO-MPI for the winter half-year are, however, quite different. There is a slight increase in  $CV_{10}$  ( $\approx 5\%$ ), mainly due to an increase in  $CV_{\text{wet}}$ .

The changes in  $CV_{10}$  in the three RCM simulations are comparable to those in the CV of monthly precipitation found in an extensive study by Räsänen (2002). In that study 19 atmosphere–ocean GCMs were considered, all forced with an increase in the atmospheric  $CO_2$  concentration of  $1\% \text{ yr}^{-1}$ . For most areas of the world an increase in the CV of monthly precipitation was found. However, for the high northern latitudes ( $50^\circ\text{N}$  and higher) a decrease was observed for autumn and winter. This decrease was associated with a relatively large increase in the mean monthly precipitation. Similar results have been found for the response of the CV of seasonal amounts in GCM climate change simulations (Rowell, 2005; Giorgi and Bi, 2005).

## Simulated changes in precipitation extremes

The nearest-neighbour resampling algorithm explained earlier was applied to the RCM control runs to generate daily sequences of precipitation and temperature for the 15 subbasins simultaneously, each with a length of 9000 years. The corrections discussed earlier were used to adjust the mean and  $CV_{10}$  of modelled precipitation amounts and the mean and standard deviation of the daily temperatures. This procedure was repeated for the A2-scenario runs, using the same corrections. In this section the distribution of the simulated 10-day maxima of basin-average precipitation for the winter half-year (flooding season) are discussed. The three panels A–C in Fig. 7 compare the Gumbel plots of these maxima in the control run and the A2-scenario run for each model configuration.

For RACMO-HC (panel A) a slight decrease is seen for return periods longer than 5 years. The change of the highest quantiles of the distribution is less than 10 mm. The effect of the increase in the mean precipitation is counterbalanced here by the decrease of  $CV_{10}$ , shown in Fig. 5. Describing the distributions of the 10-day precipitation amounts by a

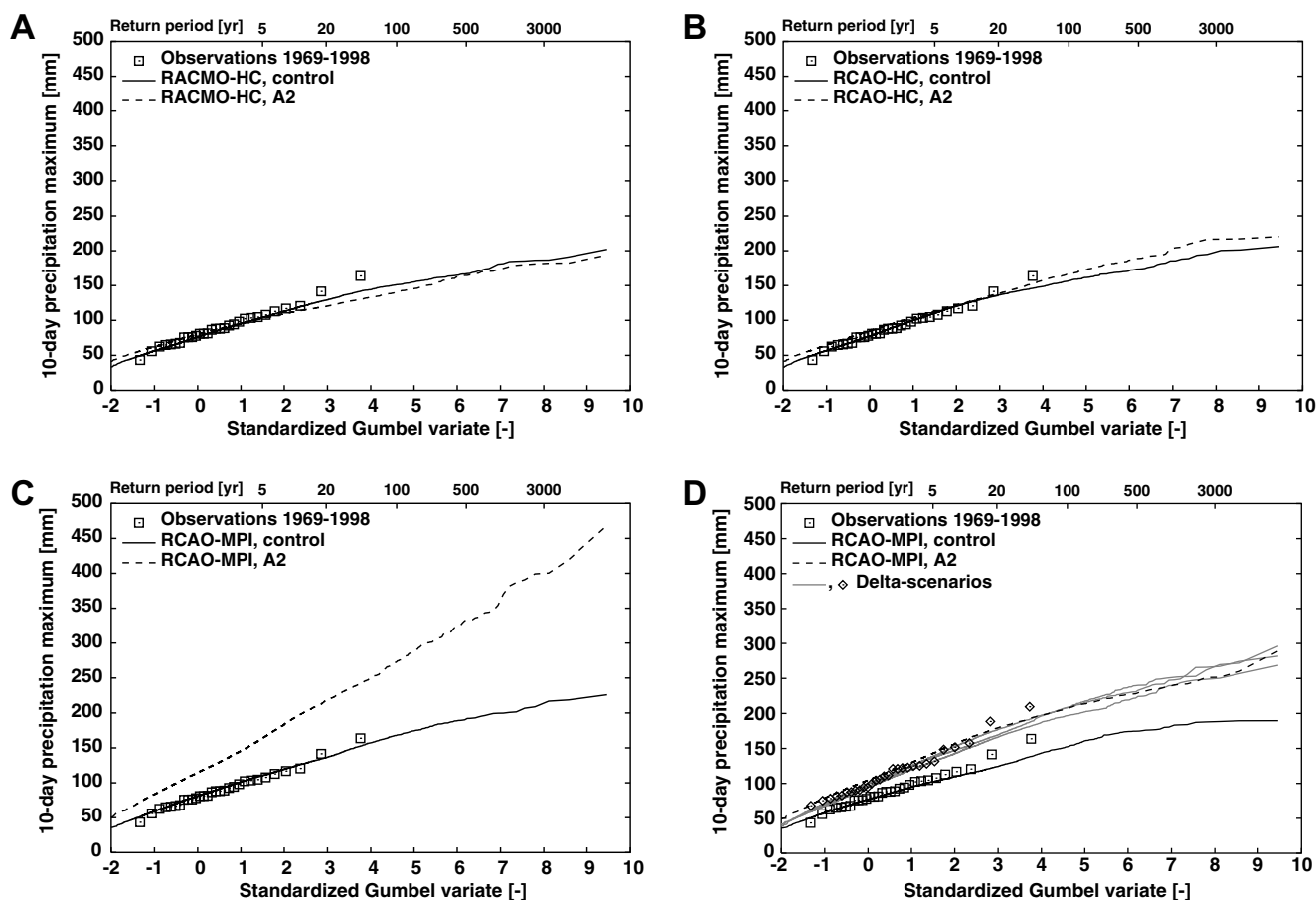


**Figure 7** Gumbel plots for the 10-day winter maxima of basin-average precipitation obtained after resampling and bias correction. Panels A–C show the results for the three model configurations: RACMO-HC, RCAO-HC and RCAO-MPI. Panel D shows the effect of limiting the bias correction on the resampled A2-scenario run from RCAO-MPI (dashed) and the ‘delta’ scenarios, obtained by applying the relative changes found in RCAO-MPI to the control runs of the three model configurations (grey) and the observations (diamonds).

square-root-normal distribution, it is demonstrated in Appendix A that the changes in the mean and  $CV_{10}$  can account for the changes in the extreme value distribution. Although a slight increase in the most extreme quantiles of 10-day precipitation is seen for RCAO-HC (panel B), the magnitude of the changes is comparable to that of RACMO-HC.

The results found for RCAO-MPI (panel C) are, however, strikingly different. The most extreme quantiles are roughly doubled. This large increase is most likely related to the nonlinear bias correction. Fig. 8 presents the ratios between the corrected and uncorrected daily precipitation amounts in the months of October and December for the Ourthe sub-basin. From the left panel it can be seen that in October the highest values in the A2-scenario run are multiplied by more than a factor of three, due to the large correction exponent  $b$  in Eq. (2) for that month (see Fig. 3). This results in daily precipitation amounts exceeding 160 mm. In some occasions, two such values occurred within a short time span, leading to extremely large 10-day amounts. For December (right panel) the correction ratios are all below 1.5.

To restrict the effect of the nonlinearity of the bias correction on large daily precipitation amounts, a modification was made to limit the ratio of corrected to uncorrected daily precipitation amounts. Using the same moving window of calendar days as for the determination of the coefficients  $a$  and  $b$  in Eq. (2), the averages  $M_{20,RCM}(i)$ ,  $i = 1, \dots, 73$  of the 20 largest daily precipitation amounts from the control run data were calculated for all 73 consecutive 5-day periods of the year. In the same way the values of  $M_{20,OBS}$  were calculated for the observations. Then the ratios  $R_{20}(i) = M_{20,OBS}(i)/M_{20,RCM}(i)$ ,  $i = 1, \dots, 73$  were determined and the largest value  $R_{max} = \max_{1 \leq i \leq 73} R_{20}(i)$  was used as an upper bound for the ratio of corrected to uncorrected rainfall amounts. This procedure was carried out for each subbasin separately. From Fig. 9 it can be seen that  $R_{max}$  varies between 1.2 and 1.9. The effect of the limited correction is shown in panel D of Fig. 7. For the control run, the quantiles of the 10-day winter maxima are somewhat lower than if no restriction would have been applied (Panel C). The

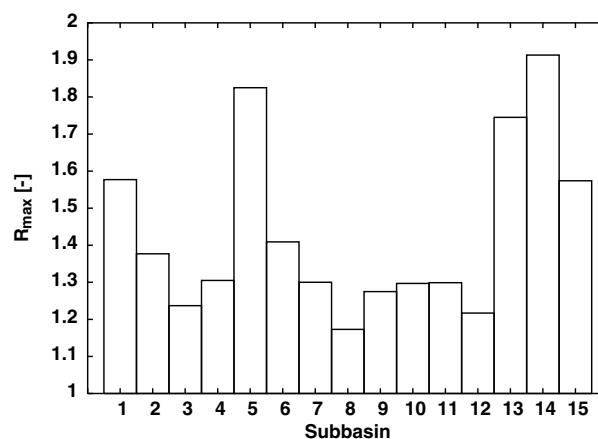


**Figure 9** The upper bound of the ratio between the corrected and uncorrected daily precipitation amount  $R_{max}$  for each subbasin. The numbers are assigned to the subbasin in downstream order. Subbasins 1–4 are located in France, subbasins 5–15 in Belgium.

agreement with the observed quantiles is, however, still satisfactory. Limiting the bias correction has a substantial effect on the extreme quantiles of the A2-scenario run. Because for the RCAO-MPI runs the average change in  $CV_{10}$  was found to be small in winter (see Fig. 5), it was expected that a ‘delta’ scenario, i.e. scaling the daily precipitation amounts of the control run by a seasonally varying factor (which represents the relative changes in the mean precipitation) may sufficiently describe the changes of the winter extremes. Therefore, the changes in the mean precipitation in RCAO-MPI were applied to the observations and the control runs from all three model configurations. Panel D of Fig. 7 shows that the 10-day winter maxima in the resulting delta scenarios resemble those from the A2-scenario run with a limited nonlinear bias correction. Thus, the change of the extreme quantiles obtained by applying the limited nonlinear bias correction to the resampled RCM runs is consistent with that expected in the case of a small change of

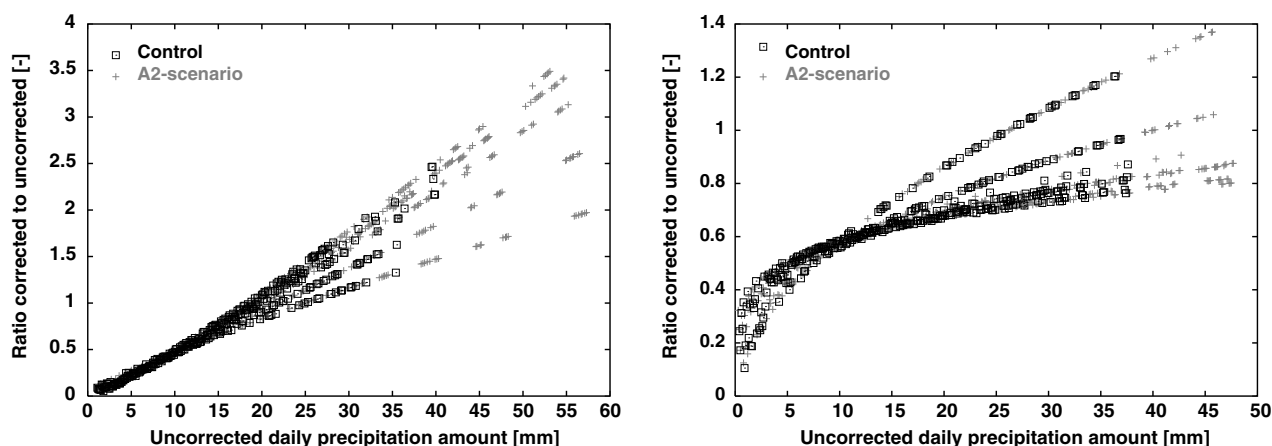


**Figure 8** Ratio between the corrected and uncorrected precipitation amounts for individual wet days in October (left) and December (right) in RCAO-MPI for the Ourthe subbasin (1588 km<sup>2</sup>). The results for both the A2-scenario run and control run are shown. The days falling within the same 5-day period in the year (and thus having the same bias-correction parameters) seem to fall along a curve in the plot.

the CV<sub>10</sub> of winter precipitation. This makes the limited correction much more plausible than the original correction.

### Estimation of changes in flood quantiles

The bias-corrected resampled series of daily precipitation and temperature discussed earlier, were used to drive hydrological simulations with the HBV rainfall–runoff model. Fig. 10 shows the Gumbel plots of the simulated winter maxima of daily discharge at Borgharen.

The flood quantiles obtained from RACMO-HC (panel A) and RCAO-HC (panel B) show roughly the same response to the A2 scenario. For both model configurations a slight decrease is seen for intermediate return periods, whereas the quantiles for the longest return periods tend to increase, in particular for RACMO-HC. For RCAO-MPI (panel C) the response of flood quantiles to the A2 scenario is much larger than for the HC-driven simulations. This is consistent with the change of the 10-day precipitation maxima. These results suggest that, at least for the winter half-year, the change of flood quantiles is more sensitive to the change of large-scale characteristics produced by the GCM, than to local effects produced by the RCM. The plots for the annual maxima (not shown) are almost identical to those shown in Fig. 10, in particular for the RCAO simulations. For RACMO there is a slight difference due to a number of large April events in the A2-scenario run.

Fig. 11 displays the relative change of the flood quantiles as a function of the standardized Gumbel variate, showing more clearly the different responses of the three model configurations to the A2 scenario. The changes for the RACMO-HC and RCAO-HC simulations are slightly different from those found by Buishand and Lenderink (2004) and Lenderink et al. (2007) for the flood quantiles of the river

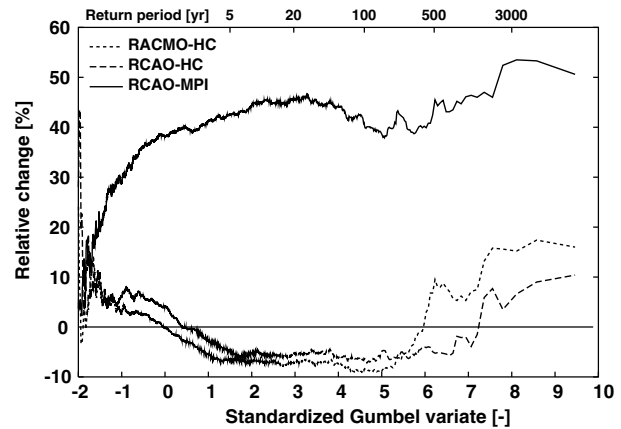


Figure 11 Relative change of the flood quantiles as a function of the standardized Gumbel variate for the three model configurations.

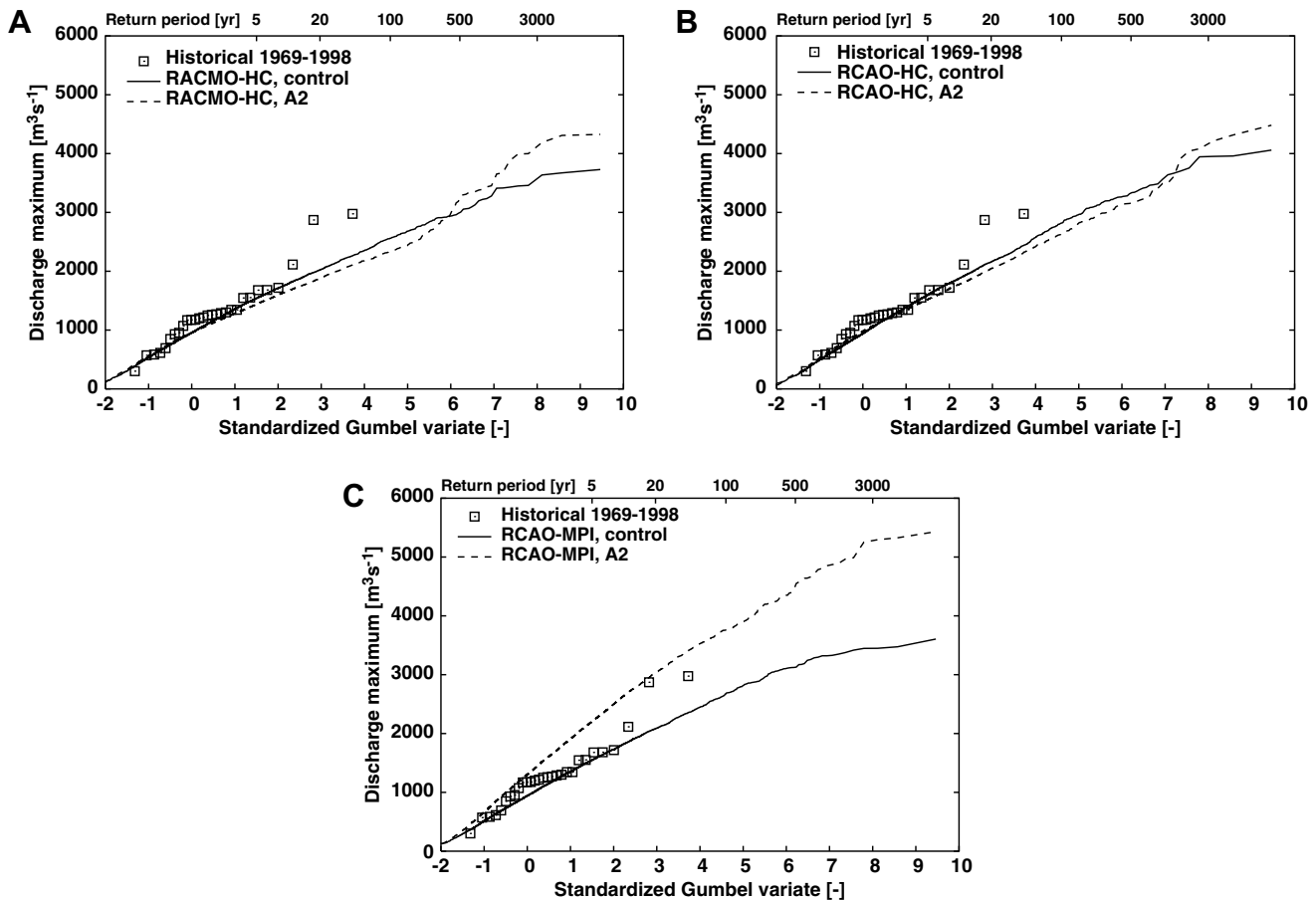
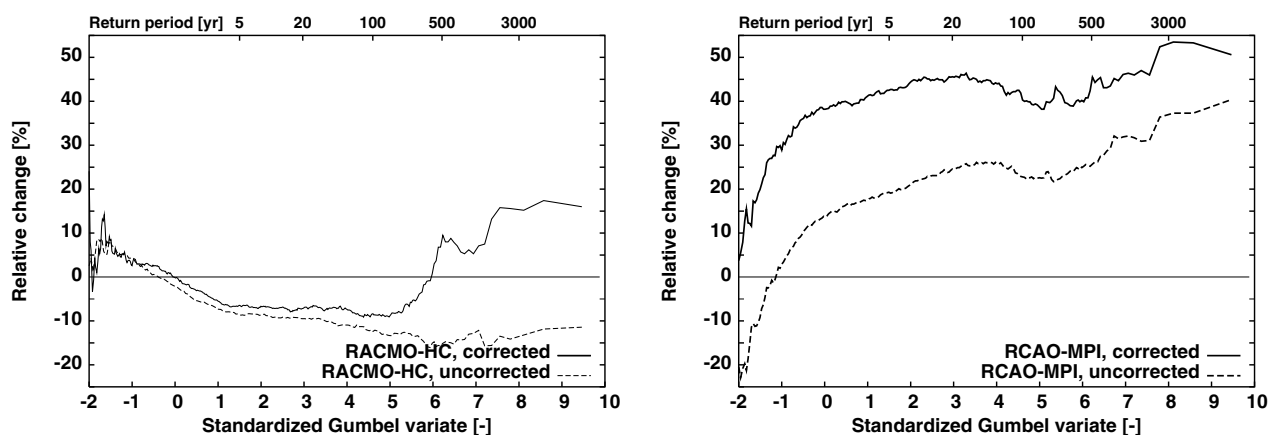


Figure 10 Gumbel plots for the maxima of daily discharge in the winter half-year for the three model configurations RACMO-HC, RCAO-HC and RCAO-MPI, the latter with the limited bias correction.



**Figure 12** Influence of the nonlinear bias correction on the relative change of the simulated flood quantiles for RACMO-HC (left panel) and RCAO-MPI (right panel).

Rhine. They found a rise of 10% in the 100-year flood. This increase is, however, less than the increase of the mean winter discharge, which is most likely related to the decrease of the CV of 10-day precipitation amounts in winter in the HC-driven runs mentioned earlier. For RCAO-MPI the relative change is between 35% and 55% over virtually the entire range of return periods. This is roughly comparable to the relative changes in the flood quantiles of the river Rhine from the delta scenario based on the UKHI experiment by Middelkoop (2000).

In order to explore the influence of the bias correction on the changes of the flood quantiles, the HBV simulations were repeated with the uncorrected resampled data from RACMO-HC and RCAO-MPI. For the control runs of these model configurations considerable biases were found in the flood quantiles (29% for RACMO-HC and 15% for RCAO-MPI for the 5-year event). The relative changes of the flood quantiles are compared in Fig. 12. For the RACMO-HC simulations (left panel) the relative change of flood quantiles is only slightly affected by the bias correction up to a return period of 100 years. For return periods beyond 500 years, the flood quantiles from the corrected data increase by about 15%, whereas those from the uncorrected data decrease by approximately the same amount. For the RCAO-MPI simulations the relative change obtained from uncorrected data is systematically lower than that obtained with the nonlinear bias correction. Thus, biases in the mean and variability of precipitation not only affect the absolute values of flood quantiles, but also their relative changes for future climate conditions. Bias correction is recommended, as it leads to realistic flood quantiles for current climate conditions.

## Discussion and conclusion

Daily precipitation and temperature from three RCM simulations (RACMO-HC, RCAO-HC and RCAO-MPI) were used to estimate the changes in flood quantiles of the river Meuse. For each model configuration, two 9000-year sequences were generated by resampling from the control run (1961–1990) and the A2-scenario run (2071–2100). These sequences were corrected for differences in the mean and

variability between the control run and observed climate. The HBV rainfall–runoff model was used to simulate the daily discharges at the gauging station Borgharen. The changes in the flood quantiles for the winter half-year were studied.

A substantial difference was found between the changes in flood quantiles from the two HC-driven simulations and those obtained from the RCAO-MPI simulations. In the HC-driven simulations there was little change in both the quantiles of extreme 10-day precipitation and the flood quantiles, despite a clear increase in the mean winter precipitation (Fig. 4). This could be explained by the fact that the increase in the mean precipitation was counteracted by a decrease in  $CV_{10}$ . By contrast, in the RCAO-MPI simulations there was little change in the  $CV_{10}$ . Mainly due to the increase in the mean precipitation amounts the quantiles of the 10-day precipitation maxima and the daily discharges increase by about 50%. The results confirm the relevance of the CV of multi-day winter precipitation as an indicator of the changes in flood quantiles, beside the change in the mean.

The change in the CV of multi-day precipitation is entirely determined by the changes in the frequency of wet days, the CV of the wet-day precipitation and the autocorrelation of daily precipitation. For the decrease of  $CV_{10}$  in the HC-driven simulations, all these factors had some influence. This decrease is consistent with that of the CV of monthly precipitation for high northern latitudes, averaged over an ensemble of GCM simulations as discussed by Räisänen (2002). However, he also reports substantial variation among the changes predicted by individual GCMs. An ensemble of RCM runs nested in different GCM runs is needed to complete the picture of the potential changes in  $CV_{10}$  and flood quantiles of the river Meuse.

It was observed that the relative change of simulated flood quantiles depends on whether or not a bias correction was used, in particular for the RCAO-MPI simulation. LB07 already showed that a nonlinear bias correction, adjusting the relative variability of multi-day precipitation amounts, is essential for a realistic simulation of extreme flood quantiles. However, for the RCAO-MPI simulation the correction had to be restricted to avoid the occurrence of unrealistically large daily precipitation amounts.

The bias correction used in this study does not take the physical causes of the precipitation bias into account. It was noted that the precipitation bias is likely to be related to biases in the atmospheric circulation. A natural alternative would be to correct for the bias in the circulation first. Nearest-neighbour methods conditioned on circulation indices might then be useful. Though such a correction has a more physical basis, its practical value is not clear. Furthermore, it is not certain whether the same correction should be applied to the circulation of the SRES A2-scenario run.

Possible trends in precipitation and temperature are disregarded in the resampling procedure. A trend could bias the selection of a new day towards the years surrounding the previous selection. For daily precipitation the trend is small compared to its variability. Daily temperature has a smaller variability and shows a considerable trend in the A2 scenario. Though the temperature in itself hardly influences the simulated extreme flows directly, the basin-averaged temperature has an influence on the resampling algorithm. The effect of the temperature trend was investigated for the A2-scenario run of RCAO-MPI. Two additional 9000-year resampling simulations were performed: one driven by the detrended temperatures and one by temperatures of which the trend had been doubled. No systematic influence of the temperature trend was found on the distribution of the maximum 10-day precipitation in winter.

It should be noted that the uncertainty in the change of the flood quantiles increases with the return period. Part of the uncertainty can be reduced by prolonging the meteorological sequences in the resampling stage. However, the uncertainty related to the limited length of the RCM runs remains. Since there is only one 30-year realization for each model experiment, this uncertainty is difficult to quantify. Furthermore, it is not clear whether the linear relation between PET and temperature derived for the current climate, is still valid in a changed climate or should be modified. However, it was shown by Lenderink et al. (2007) that the influence of assumptions regarding the potential evapotranspiration on extreme discharges are very small compared to other sources of uncertainty.

Summarizing, this study has shown that meaningful estimates of changes in extreme flood quantiles can be obtained from the daily output of RCM experiments. Apart from the change in the mean precipitation, the change in the CV of 10-day precipitation amounts emerged to be important for the Meuse basin. These changes are controlled strongly by the driving GCM. It is therefore recommended to use a comprehensive set of GCM simulations for future evaluations of the change in flood quantiles. Finally, it should be noted that bias corrections of precipitation can have a strong influence on the estimated changes of flood quantiles, but should be applied with care.

## Acknowledgements

The paper benefited from the critical comments of two anonymous reviewers. The station records and subbasin data for the Belgian part of the Meuse basin were kindly provided by the Royal Meteorological Institute of Belgium. The French station data were made available by Météo France.

The RCM data were all freely available from the PRUDENCE project.

## Appendix A. Approximation of the extreme value distribution

This appendix investigates whether the change in the quantiles of the extreme 10-day precipitation amounts in the RACMO-HC simulations can be explained by the changes in the mean and CV alone. The distribution of the 10-day precipitation amounts  $P_{10}$  can satisfactorily be described by the square-root-normal distribution, i.e.  $X = \sqrt{P_{10}}$  is normally distributed with mean  $\mu_X$  and standard deviation  $\sigma_X$ . These two parameters determine the mean  $\mu_P$  and standard deviation  $\sigma_P$  of  $P_{10}$  (Katz, 1999):

$$\mu_P = \mu_X^2 + \sigma_X^2 \quad \text{and} \quad \sigma_P^2 = 2\sigma_X^2(\sigma_X^2 + 2\mu_X^2) \quad (\text{A.1})$$

Here these relations are used to derive  $\mu_X$  and  $\sigma_X$  from  $\mu_P$  and  $\sigma_P$ :

$$\sigma_X^2 = \mu_P - \sqrt{\mu_P^2 - \frac{1}{2}\sigma_P^2} \quad \text{and} \quad \mu_X^2 = \sqrt{\mu_P^2 - \frac{1}{2}\sigma_P^2} \quad (\text{A.2})$$

The distribution of the 10-day winter maxima can be derived from the distribution of  $P_{10}$ ,  $F(x) = \text{Prob}(P_{10} \leq x)$ , using extreme-value theory. Let  $M_n$  be the maximum of the 10-day precipitation amounts in  $n$  subsequent, non-overlapping 10-day periods. Assuming independence between these precipitation amounts, the distribution of  $M_n$  is given by (Leadbetter et al., 1983):

$$H(x) = \text{Prob}(M_n \leq x) = \{F(x)\}^n \sim \exp\{-n[1 - F(x)]\} \quad (\text{A.3})$$

This distribution can be approximated by a GEV distribution (Smith, 1990):

$$H(x) \approx \exp\{-[1 - \theta(x - \mu)/\sigma]^{1/\theta}\} \quad (\text{A.4})$$

The parameters  $\mu$ ,  $\sigma$  and  $\theta$  of  $H$  depend on  $n$ . The location parameter  $\mu$  is obtained as the  $1/n$  upper quantile of  $F$ , i.e.

$$1 - F(\mu) = 1/n \quad (\text{A.5})$$

Subsequently, the scale parameter  $\sigma$  and the shape parameter  $\theta$  are calculated using the first and second derivatives  $F'$  and  $F''$  of  $F$  in  $\mu$ :

$$\sigma = \frac{1}{n} \frac{1}{F'(\mu)} \quad \text{and} \quad \theta = \sigma \frac{F''(\mu)}{F'(\mu)} + 1 \quad (\text{A.6})$$

This approximation is known as the penultimate distribution. Since the winter half-year is considered here, a value of 18.5 was chosen for  $n$ . Because  $(\sqrt{P_{10}} - \mu_X)/\sigma_X$  is assumed to be standard-normally distributed, the solution of Eq. (A.5) is given by

$$\mu = \left[ \mu_X + \sigma_X \Phi^{-1} \left( 1 - \frac{1}{n} \right) \right]^2 \quad (\text{A.7})$$

where  $\Phi^{-1}$  is the inverse of the standard normal distribution function. The probability density  $F'$  and its derivative  $F''$  in  $\mu$ , which are required to calculate the scale parameter  $\sigma$  and the shape parameter  $\theta$ , are given by

$$F'(\mu) = \frac{1}{2\sigma_X\sqrt{\mu}} \varphi(z) \quad (\text{A.8})$$

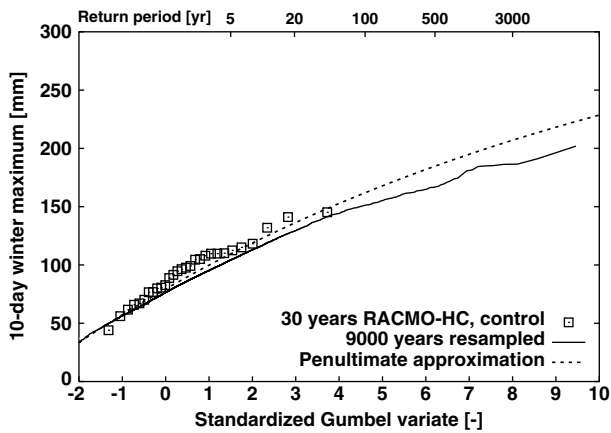


**Figure A.1** Penultimate approximation of the distributions of extreme 10-day basin-average precipitation totals for the winter half-year (dashed), compared with the empirical quantiles from a 9000-year resampled series (solid) and those of the 30-year RCM control run (squares).

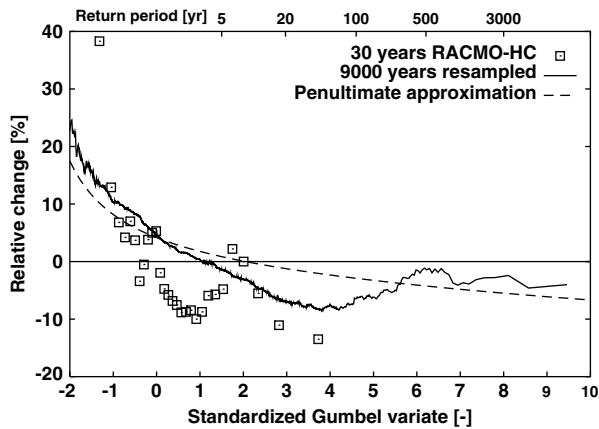


**Figure A.2** Change in the quantiles of the 10-day winter maxima of basin-average precipitation, extracted from the bias-corrected 30-year control run and A2-scenario run of RACMO-HC (squares) and from the corresponding 9000-year resampled sequences (solid) and penultimate approximations (dashed) derived from these runs.

and

$$F''(\mu) = -\frac{1}{4\mu\sigma_X} \varphi(z) \left( \frac{1}{\sqrt{\mu}} + \frac{z}{\sigma_X} \right) \quad (\text{A.9})$$

where  $\varphi$  denotes the standard normal density and  $z = (\sqrt{\mu} - \mu_X) / \sigma_X$ .

The 10-day precipitation maxima considered in this paper (Fig. 7) refer to overlapping 10-day periods. These maxima are generally larger than those for consecutive 10-day periods. To account for this discrepancy, the location parameter  $\mu$  and the scale parameter  $\sigma$  were multiplied by 1.13, which implies that the quantiles of the distribution of  $M_n$  change with the same factor. The factor 1.13 is due to Hershfield (1961). It has been used to adjust the quantiles of clock-hour and 1-day maxima to the corresponding quantiles of sliding 60-min and 24-h maxima, respectively.

For the 10-day precipitation amounts in winter from the control run of RACMO-HC Fig. A.1 compares the Gumbel plots of the 30-year run and the 9000-year resampled series with the penultimate approximation. For the penultimate approximation,  $\mu = 79.4$  mm,  $\sigma = 21.2$  mm and  $\theta = 0.0755$ . It is seen that this GEV distribution slightly overestimates the quantiles of the resampled maxima, though there is a good agreement with those of the 30-year RCM run.

Fig. A.2 shows the relative change of the quantiles of the 10-day winter maxima. The change derived from the penultimate approximation roughly agrees with that found from the resampled sequences. This indicates that the changes of the mean and  $CV_{10}$  indeed can account for the change of the quantiles of the maxima in winter.

## References

- Bárdossy, A., Zehe, E., 2002. Hydrological impact of climate change on the river Rhine. Report of the IRMA-SPONGE project "Development of flood management strategies for the Rhine and Meuse basins in the context of integrated river management". Institute of Hydraulic Engineering (IWS), University of Stuttgart, Stuttgart, Germany.
- Booij, M.J., 2002. Appropriate modelling of climate change impacts on river flooding. PhD thesis. University of Twente, Enschede.
- Booij, M.J., 2005. Impact of climate change on river flooding assessed with different spatial model resolutions. *Journal of Hydrology* 303, 176–198.
- Buishand, T.A., Lenderink, G., 2004. Estimation of future discharges of the river Rhine in the SWURVE project. Technical report TR-273. Royal Netherlands Meteorological Institute (KNMI), De Bilt, The Netherlands.
- Bultot, F., Coppens, A., Dupriez, G.L., Gellens, D., Meulenberghs, F., 1988. Repercussions of a CO<sub>2</sub> doubling on the water cycle and on the water balance – a case study for Belgium. *Journal of Hydrology* 99, 319–347.
- Christensen, J.H., Christensen, O.B., 2007. A summary of the PRUDENCE model projections of changes in the European climate by the end of this century. *Climatic Change* 81, 7–30. doi:10.1007/s10584-006-9210-7.
- Cox, D.R., Lewis, P.A.W., 1966. *The Statistical Analysis of Series of Events*. Chapman and Hall, London, UK.
- de Wit, M.J.M., van den Hurk, B., Warmerdam, P.M.M., Torfs, P.J.J.F., Roulin, E., van Deursen, W.P.A., 2007. Impact of climate change on low-flows in the river Meuse. *Climatic Change* 82, 351–372. doi:10.1007/s10584-006-9195-2.
- Gellens, D., Roulin, E., 1998. Streamflow response of Belgian catchments to IPCC climate change scenarios. *Journal of Hydrology* 210, 242–258.
- Giorgi, F., Bi, X., 2005. Regional changes in surface climate interannual variability for the 21st century from ensembles of global model simulations. *Geophysical Research Letters* 32, L13701. doi:10.1029/2005GL023002.
- Grabs, W. (Ed.), 1997. *Impact of climate change on hydrological regimes and water resources management in the Rhine basin*. CHR Report I-16. Secretariat of the International Commission for the Rhine basin (CHR), Lelystad, The Netherlands.
- Hershfield, D.M., 1961. *Rainfall frequency atlas of the United States for durations from 30 minutes to 24 hours and return periods from 1 to 100 years*. Weather Bureau Technical Paper 40. US Department of Commerce, Washington, DC, USA.
- Jacob, D., et al., 2007. An inter-comparison of regional climate simulations for Europe: model performance in present-day climate. *Climatic Change* 81, 31–52. doi:10.1007/s10584-006-9213-4.

- Jones, R., Murphy, J., Hassel, D., Taylor, R., 2001. Ensemble mean changes in the simulation of the European climate of 2071–2100 using the new Hadley Centre regional modelling system HadAM3H/HadRM3H. Hadley Centre Report. Hadley Centre, Met Office, Bracknell, UK.
- Katz, R.W., 1999. Moments of power transformed time series. *Environmetrics* 10, 301–307.
- Kay, A.L., Jones, R.G., Reynard, N.S., 2006. RCM rainfall for UK flood frequency estimation. II: climate change results. *Journal of Hydrology* 318, 163–172.
- Kleinn, J., Frei, C., Gurtz, J., Lüthi, D., Vidale, P.L., Schär, C., 2005. Hydrologic simulations in the Rhine basin driven by a regional climate model. *Journal of Geophysical Research* 110. doi:10.1029/2004JD005143.
- Kwadijk, J., Rotmans, J., 1995. The impact of climate change on the river Rhine: a scenario study. *Climatic Change* 30, 397–426.
- Leadbetter, M.R., Lindgren, G., Rootzén, H., 1983. *Extremes and Related Properties of Random Sequences and Processes*. Springer-Verlag, New York.
- Leander, R., Buishand, T.A., 2007. Resampling of regional climate model output for the simulation of extreme river flows. *Journal of Hydrology* 332, 487–496.
- Leander, R., Buishand, T.A., Aalders, P., de Wit, M.J.M., 2005. Estimation of extreme floods of the river Meuse using a stochastic weather generator and a rainfall–runoff model. *Hydrological Sciences Journal* 50, 1089–1103.
- Lenderink, G., van den Hurk, B.J.J.M., van Meijgaard, E., van Ulden, A.P., Cuijpers, H., 2003. Simulation of present-day climate in RACMO2: first results and model developments. Technical Report TR-252. Royal Netherlands Meteorological Institute (KNMI), De Bilt, The Netherlands.
- Lenderink, G., Buishand, T.A., van Deursen, W., 2007. Estimates of future discharges of the river Rhine using two scenario methodologies: direct versus delta approach. *Hydrology and Earth System Sciences* 11, 1145–1159.
- Lindström, G., Johansson, B., Persson, M., Gardelin, M., Bergström, S., 1997. Development and test of the distributed HBV-96 hydrological model. *Journal of Hydrology* 201, 272–288.
- Middelkoop, H. (Ed.), 2000. The impact of climate change on the river Rhine and the implications for water management in the Netherlands. Summary report of the NRP project 952210. RIZA Report 2000.010. Institute for Inland Water Management and Waste Water Treatment (RIZA), Lelystad, The Netherlands.
- Middelkoop, H., Daamen, K., Gellens, D., Grabs, W., Kwadijk, J.C.J., Lang, H., Parmet, B.W.A.H., Schädler, B., Schulla, J., 2001. Impact of climate change on hydrological regimes and water resources management in the Rhine basin. *Climatic Change* 49, 105–128. doi:10.1023/A:1010784727448.
- Prudhomme, C., Reynard, N., Crooks, S., 2002. Downscaling of global climate models for flood frequency analysis: where are we now? *Hydrological Processes* 16, 1137–1150.
- Räisänen, J., 2002. CO<sub>2</sub>-induced changes in interannual temperature and precipitation variability in 19 CMIP2 experiments. *Journal of Climate* 15, 2395–2411.
- Räisänen, J., Hansson, U., Ullerstig, A., Döscher, R., Graham, L.P., Jones, C., Meier, H.E.M., Samuelsson, P., Willén, U., 2004. European climate in the late twenty-first century: regional simulations with two driving global models and two forcing scenarios. *Climate Dynamics* 22, 13–31.
- Rajagopalan, B., Lall, U., 1999. A *k*-nearest-neighbor simulator for daily precipitation and other weather variables. *Water Resources Research* 35, 3089–3101.
- Roeckner, E., Bengtsson, L., Feichter, J., Lelieveld, J., Rodhe, H., 1999. Transient climate change simulations with a coupled atmosphere–ocean GCM including the tropospheric sulfur cycle. *Journal of Climate* 12, 3004–3032.
- Rowell, D.P., 2005. A scenario of European climate change for the late twenty-first century: seasonal means and interannual variability. *Climate Dynamics* 25, 837–849.
- Shabalova, M.V., van Deursen, W.P.A., Buishand, T.A., 2003. Assessing future discharge of the river Rhine using regional climate model integrations and a hydrological model. *Climate Research* 23, 233–246.
- Smith, R.L., 1990. Extreme value theory. In: Ledermann, W. et al. (Eds.), *Handbook of Applicable Mathematics, Supplement*. Wiley, Chichester, pp. 437–472.
- Tu, M., 2006. Assessment of the effects of climate variability and land use change on the hydrology of the Meuse river basin. PhD thesis. UNESCO-IHE, Delft, The Netherlands.
- van Ulden, A.P., Lenderink, G., van den Hurk, B.J.J.M., van Meijgaard, E., 2007. Circulation statistics and climate change in Central Europe: PRUDENCE simulations and observations. *Climatic Change* 81, 179–192. doi:10.1007/s10584-006-9212-5.